university of groningen

faculty of mathematics and natural sciences

Modelling the Oryon watermill using porous screens

Bachelor Project Mathematics

February 2017

Student: L.C. (Lisa) Bogers

First supervisor: Prof. dr. ir. R.W.C.P. (Roel) Verstappen

Second supervisor: Dr. ir. R. (Roel) Luppes

Modelling the Oryon watermill using porous screens

Lisa C. Bogers

February 17, 2017

Abstract

The Oryon watermill produces power from low-velocity fluid flow in shallow rivers. The watermill consists of three rotorarms each containing several lamellae, through which momentum is transferred from the water to the rotor. A numerical model of this would be very computationally expensive. In this research, the possibility of modelling the lamellae using porous screens is investigated. Several ways of modelling are discussed, such as a potential flow model. Integral mass- and momentum balances are established for both the lamellae and the porous screen. For the porous screen a source term is added. The balances are then compared to find a relation between the porosity of the screen and the opening angle of the lamellae. This relation is checked numerically using an OpenFOAM model.

Contents

1 Introduction **4**

2 Potential flow model for lamellae **6**
2.1 Stream function 6
2.2 Complex velocity potential 6
2.3 Flow past one cylinder 7
2.4 Flow past one lamella 8
2.5 Forces on a lamella 9
2.6 Momentum transfer to one lamella 10
2.7 Several lamellae 11

3 Mass- and momentum balances for lamellae **12**
3.1 Control volume 12
3.2 Conservation of mass 13
3.3 Momentum balance 15
3.3.1 Inviscid flow 15
3.3.2 Viscous flow 16
3.4 Momentum transfer for one lamella 17
3.5 Momentum transfer for several lamellae 18

4 Physical flow through a porous screen **19**
4.1 Porosity 19
4.2 Pressure drop 19
4.3 Deflection 21
4.4 Forces on a porous screen 22
4.5 Mass flow 23
4.6 Momentum transfer to a porous screen 24

5 Mass- and momentum balances for a porous screen **25**
5.1 Control volume 25
5.2 Source term 26
5.3 Forces 27
5.4 Finding coefficient d 28

6 Relation between porosity and opening angle **30**
6.1 Mass flow 30
6.2 Momentum transfer 31

7 Numerical model **32**
7.1 Results 32
7.2 Notes 34

8 Conclusion **35**

9 Discussion **36**

1 Introduction

The Oryon watermill is a water generator that can be used for power production in shallow rivers and canals. The watermill consists of a three-armed rotor that is vertically mounted in a fully submerged shrouding. The three-armed rotor can be seen in Figure 1. One of the distinguishing features of the generator is the fact that momentum is not directly transferred from the water flow to the rotor, but through a set of 12 hinged lamellae. These lamellae open and close under the hydrodynamic load. This partially unrestricted movement reduces drag, i.e. undesired momentum transfer during the recovery phase of the rotorarms. The geometry and configuration of the lamellae has a significant influence on the performance of the generator.

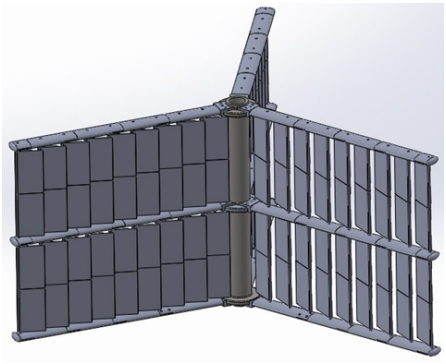

Figure 1: The Oryon watermill, consisting of three rotorarms each containing several lamellae ([13])

The performance of the watermill can be studied using a computational model. However, the complexion of such a model will make the evaluation of a single flow condition very computationally intensive. Therefore, simpler ways of modelling the lamellae have to be considered if a large number of flow conditions have to be analyzed. One of those alternative, simpler ways of modelling might be to use porous screens. This alternative 'porous screen model' will be determined and analyzed in this research.

In such a porous screen model the (sets of) individually moving lamellae can be replaced by porous screens that are fixed to the rotorarms. This porous screen model can be compared to the original 'lamellae model' to find a relation between the porosity of the porous screen and the opening angle of the lamellae. For the lamellae, it is in this case assumed that they are in a fixed position, instead of moving in accordance with the flow. Consequently, the problem discussed in this research will be more generic than the real situation.

There are several possible ways of modelling the porous screen and the lamellae. For example, a potential flow model might be used to model uniform potential flow past several lamellae. For a simplified situation, integral mass- and momentum balances can be established for both the lamellae and the porous screen. Both of these options will be considered in this report. After composing analytical models for both the lamellae and the porous screen, a relation between the porosity of the porous screen and the opening angle of a lamella can probably be determined. This relation can be verified using a numerical model in OpenFOAM.

Hence, the purpose of this research is to analytically find a relation between the porosity of the porous screen and the opening angle of the lamellae, which can be validated numerically. Then after considering the accuracies and shortcomings of the lamellae model and the porous screen model, a conclusion can be drawn about the possibility to use porous screens instead of lamellae for modelling the Oryon watermill.

2 Potential flow model for lamellae

Firstly, a potential flow model will be used for modelling the flow (see [8]). Potential flow is irrotational flow of a homogeneous, inviscid or viscous (for now inviscid), incompressible fluid. The velocity field then satisfies $\nabla \cdot \mathbf{v} = 0$ and $\nabla \times \mathbf{v} = 0$. There exists a scalar velocity potential Φ such that $\mathbf{v}$ is equal to the gradient of Φ:

$$\mathbf{v} = \nabla\Phi$$

From the conservation of mass, $\nabla \times \mathbf{v} = 0$, it follows that Φ has to satisfy the two-dimensional potential equation:

$$\nabla \cdot \nabla\Phi \equiv \Delta\Phi \equiv \Phi_{xx} + \Phi_{yy} = 0$$

In two-dimensional flow, all quantities are only dependent on the two spacial coordinates x and y (and possibly time t). This gives the following equations:

$$\frac{\partial u}{\partial x} + \frac{\partial v}{\partial y} = 0, \quad \frac{\partial u}{\partial y} - \frac{\partial v}{\partial x} = 0$$

where u and v are the velocity components in respectively the x- and the y-direction. From the equations above, it follows that u and v are both potential functions: $u_{xx} + u_{yy} = v_{xx} + v_{yy} = 0$.

2.1 Stream function

Since $\nabla \cdot \mathbf{v} = 0$, there exists a vector field $\mathbf{A}$ such that $\mathbf{v} = \nabla \times \mathbf{A}$. In other words, $\mathbf{v}$ is the rotation of $\mathbf{A}$. For at two-dimensional velocity vector $\mathbf{v} = (u, v, 0)$, we can choose the rotation vector $\mathbf{A} = (0, 0, \psi)$. This function ψ is then called the stream function. From $\mathbf{v} = \nabla \times \mathbf{A} = (\psi_y - \psi_x, 0)$ it follows that $\psi_y = u$ and $\psi_x = -v$. From $\frac{\partial u}{\partial y} - \frac{\partial v}{\partial x} = 0$, it then follows that ψ has to be a potential function: $\psi_{xx} + \psi_{yy} = 0$. The curves $\psi =$ constant represent the streamlines and the curves $\phi =$ constant represent the equipotential lines.

2.2 Complex velocity potential

The functions ψ (the stream function) and ϕ are related through the well-known Cauchy-Riemann equations from complex function theory ([8]):

$$\phi_x = \psi_y, \quad \phi_y = -\psi_x (= v)$$

The real and imaginary parts of an analytic function of the complex variable $z = x + iy$ should satisfy these equations. In other words, if the complex velocity potential $\chi = \phi + i\psi$ is an analytic function of z, then ϕ and ψ satisfy $\phi_x = \psi_y$ and $\phi_y = -\psi_x$. Every analytic function $\chi(z)$ corresponds to a two-dimensional

potential flow. However, this does not mean that this flow is always physically interesting. The meaning of $\chi'(z)$ follows from taking the derivative to z in the x- or y-direction ([8]):

$$\frac{d\chi}{dz} = \frac{\partial \chi}{\partial x} = \frac{\partial \phi}{\partial x} + i\frac{\partial \psi}{\partial x} = u - iv \equiv w(z)$$

Similarly,

$$\frac{d\chi}{dz} = \frac{\partial \chi}{\partial (iy)} = \frac{1}{i}\frac{\partial \phi}{\partial y} + \frac{\partial \psi}{\partial y} = u - iv \equiv w(z)$$

The function $w(z)$ is called the complex velocity.

It is assumed that the potential flow is uniform. If the flow makes an angle α with the x-axis, the complex velocity is given by:

$$w(z) = u - iv = U\cos\alpha - iU\sin\alpha = Ue^{-i\alpha}$$

The complex velocity potential is then given by

$$\chi = Uze^{-i\alpha} \tag{1}$$

This can be used to describe potential flow past one cylinder and that can be expanded to potential flow past a flat plate. This will be done in the next sections.

2.3 Flow past one cylinder

For the flow past a cylinder without circulation, the complex potential χ is according to [8] given by

$$\chi(z) = U\left(z + \frac{a^2}{z}\right) \tag{2}$$

which gives the following complex velocity:

$$w(z) = \frac{\partial \chi}{\partial z} = U\left(1 - \frac{a^2}{z^2}\right) \tag{3}$$

Since $w(\pm a) = 0)$, the stagnation points (where the flow velocity is zero) are at $z = \pm a$. If circulation is added to the flow, a vortex in $z = 0$ with strength $\Gamma > 0$ is added to (2):

$$\chi(z) = U\left(z + \frac{a^2}{z}\right) + \frac{i\Gamma}{2\pi}\ln z \tag{4}$$

This is a flow with circulation $C = -\Gamma$ along every contour that is included in $z = 0$.

2.4 Flow past one lamella

Potential flow past a cylinder is easiest to model. For other obstacles it will be difficult to find the complex potential χ. Therefore, we make use of conformal mappings. The idea behind conformal mappings is that the mapping of an analytic function representing a flow, is a flow. If we take an analytic mapping $\zeta = g(z)$, then χ transforms in the following way:

$$\chi(\zeta) = \chi(g(\zeta)) = (\chi \circ g)(z) = \chi^*(z)$$

The complex velocity w in the z-plane can then be calculated using the chain rule:

$$w = \frac{d\chi^*}{dz} = \frac{d\chi}{d\zeta}\frac{d\zeta}{dz} = g'(z)\frac{d\chi}{d\zeta} \tag{5}$$

The Joukowsky transformation maps a cylinder to a flat plate ([8]). This mapping is given by

$$z = \zeta + \frac{a^2}{\zeta}, \quad a \in \mathbb{R}, a > 0 \tag{6}$$

where $\zeta = ae^{i\varphi}$. The circle in the ζ-plane with radius a and center in the origin is mapped onto the segment $[-2a, 2a]$ of the real axis in the z-plane:

$$z = a\left(e^{i\varphi} + e^{-i\varphi}\right) = 2a\cos\varphi \quad (0 \leq \varphi \leq 2\pi) \tag{7}$$

Using this Joukowsky transformation, the flow around a lamella (a flat plate) can be found from the flow around a cylinder and vice versa. Now, we want to use this to determine the flow around an inclined flat plate.

The stream function for flow around an inclined flat plate can be found using the Joukowsky transformation and the stream function for flow around a cylinder with radius a. According to [8], the relation between the flow around a cylinder in the ζ-plane and the flow around a cylinder with angle of incidence α in the ζ-plane is given by

$$\zeta = \tilde{\zeta}e^{i\alpha} \tag{8}$$

This relation can also be written as

$$\tilde{\zeta} = \zeta e^{-i\alpha} \tag{9}$$

The relation between the flow around a flat plate with inclination angle α in the z-plane and the flow around a cylinder with inclination angle α in the ζ-plane is given by

$$z = \zeta + \frac{a^2}{\zeta} \tag{10}$$

By implementing (9) into (4), the stream function for the flow around a cylinder with angle α is found:

$$\chi(\tilde{\zeta}) = U\left(\tilde{\zeta} + \frac{a^2}{\tilde{\zeta}}\right) + \frac{i\Gamma}{2\pi}\ln\zeta = U\left(\zeta e^{-i\alpha} + \frac{a^2}{\zeta}e^{i\alpha}\right) + \frac{i\Gamma}{2\pi}\ln\zeta = \chi(\zeta) \tag{11}$$

Now using (10), we can get the stream function in the z-plane. Since the inverse of the Joukowsky function is difficult to find, the function $\chi^*(z)$ will be expressed in terms of ζ, with the function $z = g(\zeta)$. The velocity potential w can be obtained using (5),

$$w = \frac{d\chi^*}{dz} = \frac{d\chi}{d\zeta}\frac{d\zeta}{dz} = \frac{d\chi}{d\zeta}\left(\frac{dz}{d\zeta}\right)^{-1} = \left(U\left(e^{-i\alpha} + \frac{a^2}{\zeta^2}e^{i\alpha}\right) + \frac{i\Gamma}{2\pi\zeta}\right)\left(1 - \frac{a^2}{\zeta^2}\right)^{-1} \tag{12}$$

with $z = \zeta + \frac{a^2}{\zeta^2}$. Thus, the complex velocity of flow around a lamella with angle of incidence α is given by equation (12).

The points $z = 2a\cos\varphi$ on the flat plate correspond to the points $\zeta = ae^{i\varphi}$ on the circle. Implementing $\zeta = ae^{i\varphi}$ into equation (12) gives the following expression for complex velocity at the flat plate:

$$w_{plate} = \left(U\left(e^{-i\alpha} - e^{i(\alpha-2\varphi)}\right) + \frac{i\Gamma}{2\pi a}e^{-i\varphi}\right)\left(1 - e^{-2i\varphi}\right)^{-1} = \frac{U\sin(\varphi-\alpha) + \frac{\Gamma}{4\pi a}}{\sin\varphi} \tag{13}$$

For $\varphi = 0$, the velocity at the plate has to be finite: $|w_{plate}| < \infty$. From this, it follows that the numerator of the expression for w_{plate} has to be zero:

$$U\sin(0-\alpha) + \frac{\Gamma}{4\pi a} = 0$$

This gives us the expression for the strength of the vortex, which is $\Gamma = 4\pi U a \sin\alpha$.

Thus, the complex velocity of flow around a lamella with angle of incidence α is given by equation (12). The complex velocity at the plate is given by equation (13). In the next section the forces on the lamella will be determined.

2.5 Forces on a lamella

According to [8], the forces on the plate can be determined using the first law of Blasius:

$$X - iY = \frac{1}{2}i\rho\oint\left(\frac{d\chi*}{dz}\right)^2 dz = \frac{1}{2}i\rho\oint\left(\frac{d\chi}{dz}\right)^2\left(\frac{dz}{d\zeta}\right)^{-1}\frac{dz}{d\zeta}d\zeta \tag{14}$$

where the direction of the force X is the positive x-direction, which is in this case parallel to the lamella. Naturally, the direction of the force Y is the positive y-direction, which is perpendicular to the lamella. It holds that

$$\frac{d\chi}{d\zeta} = U\left(e^{-i\alpha} - \frac{a^2}{\zeta^2}e^{i\alpha}\right) + \frac{i\Gamma}{2\pi\zeta}$$

and

$$\left(\frac{dz}{d\zeta}\right)^{-1} = \left(1 - \frac{a^2}{\zeta^2}\right)^{-1} \approx 1 + \frac{a^2}{\zeta^2} + \frac{a^4}{\zeta^4} + ...$$

Writing out the asymptotical development of the integrand gives

$$\left(\frac{d\chi}{dz}\right)^2 \left(\frac{dz}{d\zeta}\right)^{-2} = U^2 e^{-2i\alpha} + \left(U e^{-i\alpha} \frac{i\Gamma}{\pi}\right) \frac{1}{\zeta} + h.o.t. \tag{15}$$

The only term in the integrand that is not zero is the term that behaves like $\frac{1}{\zeta}$ for $|\zeta| \to \infty$. Hence, integrating the integrand in equation (15) gives

$$X - iY = \frac{1}{2} i\rho \oint \left(\frac{d\chi}{dz}\right)^2 \left(\frac{dz}{d\zeta}\right) - 1 d\zeta = 2\pi i \left(\frac{1}{2} i\rho \left(U e^{-i\alpha} \frac{i\Gamma}{\pi}\right)\right) = -i\rho U \Gamma e^{-i\alpha} \tag{16}$$

This gives $X = -\rho U \Gamma \sin\alpha$ and $Y = \rho U \Gamma \cos\alpha$. Note that the direction of X is parallel to the inclined plate and the direction of Y is perpendicular to the inclined plate. The lamellae do not transfer momentum from the water to the water mill immediately, but through the rotorarms. Therefore, the force that contributes to the momentum transfer is the force perpendicular to the rotorarm. To determine this force, we need to know (or assume) the relation between the angle of the rotorarm and the opening angle of the lamella. For now, we will assume that the rotorarm is in the direction perpendicular to the upstream flow velocity. Then, the force perpendicular to the rotorarm (consisting of one lamella) is given by

$$\vec{F}_\perp = X \cos\alpha = -\rho U \Gamma \sin\alpha \cos\alpha = -\rho U^2 4\pi a \sin^2\alpha \cos\alpha \tag{17}$$

where $\Gamma = 4\pi U a \sin\alpha$. The momentum transfer to the rotorarm consisting of one lamella will be determined in the next section.

2.6 Momentum transfer to one lamella

According to [8], the torque acting on one lamella (flat plate) about the origin is given by

$$\tau(0,0) = Re\left[-\frac{1}{2}\rho \oint z \left(\frac{d\chi^*}{dz}\right)^2 dz\right] = Re\left[-\frac{1}{2}\rho \oint \left(\frac{d\chi^*}{dz}\right)^2 \left(\frac{dz}{d\zeta}\right)^{-1} \left(\zeta + \frac{a^2}{\zeta}\right) d\zeta\right]$$

This can also be written as

$$\tau(0,0) = Re\left[-\frac{1}{2}\rho \left(2\pi i \left(2U^2 a^2 e^{-2i\alpha} - 2U^2 a^2 - \frac{\Gamma^2}{4\pi^2}\right)\right)\right]$$

Which simplifies to

$$\tau(0,0) = -2\pi\rho U^2 a^2 \sin(2\alpha) \tag{18}$$

From this, it can be seen that the vortex strength Γ does not influence the torque.

The angular momentum $\vec{L}$ of one lamella is given by

$$\frac{d\vec{L}}{dt} = \vec{\tau} \tag{19}$$

Using this equation, the angular momentum transfer to one lamella can be determined. Adding the momenta of the several lamellae on one rotorarm will then give the angular momentum transfer to the whole rotorarm. The angular momentum transfer to one lamella is given by

$$\vec{L} = \int_{t_0}^{t_{eind}} \vec{\tau} dt = \int_0^t -2\pi\rho U^2 a^2 \sin(2\alpha) dt = -2\pi\rho U^2 a^2 \sin(2\alpha) t \tag{20}$$

It is assumed that U is uniform over the width of the lamella.

2.7 Several lamellae

The Oryon watermill consists of three rotorarms, each of which consists of 12 lamellae. Therefore, it would be useful to model the flow past several lamellae. However, this is easier said than done. An analytical model for uniform flow past several cylinders is described in [9]. A Joukowsky transformation can be used to transform this from cylinders to flat plates. The mapping $z(\zeta)$ would then be a double-connected Schwarz Christoffel mapping from the annulus. The derivative $\frac{\partial z}{\partial \zeta}$ can then be written down explicitly using the Schottky-Klein prime function.

The Schwarz Christoffel mappings and the Schottky-Klein prime function are quite involved ([10]). Hence, building a potential flow model for this research would be too time-consuming. That is why in this research mass- and momentum balances will be used, as can be seen in the next chapter. Naturally, this does not mean that the problem can not be solved using a potential flow model.

3 Mass- and momentum balances for lamellae

Constructing a potential flow model for the research problem appears to be too ambitious. Therefore, mass- and momentum balances will now be used. Using those balances, the mass flow through the lamellae, the forces on the lamellae and the momentum transfer to the rotorarms will be determined.

3.1 Control volume

A control volume is an arbitrary volume in space through which the fluid, in this case water, flows ([2]). For a control volume basic laws such as conservation of mass and the momentum balance can be written. It is important to be careful in selecting a control volume, since the choice greatly affects the mathematical laws that are used. A control volume for this problem will be assigned to be able to compose the mass- and momentum balances. Firstly, the control volume for one lamella can be seen in Figure 2 and can be described in the following way:

The angle between the horizontal (x-direction) and the lamella is α. The control volume is a parallellogram. The upside of the parallelogram is formed by the lamella. The underside is of course parallel to lamella and it is assumed to be a streamline. The first control surface CS_1, through which the fluid enters the control volume, is given by the left side of the parallellogram. The second control surface CS_2, through which the fluid leaves the control volume, is given by the right side of the parallellogram.

Since the fluid flow is not restricted to any kind of jet, it flows into the control volume over the whole surface area CS_1 and out of the control volume over the whole surface area CS_2. The surface areas $A_1 = CS_1$ and $A_2 = CS_2$ can be expressed using the area of the lamella, A_{plate}. When α is the angle between the lamella and the horizontal, it is trivial that

$$A_1 = A_{plate} \sin \alpha = A_2$$

These expressions will be used in the following analyses of the mass- and momentum balances.

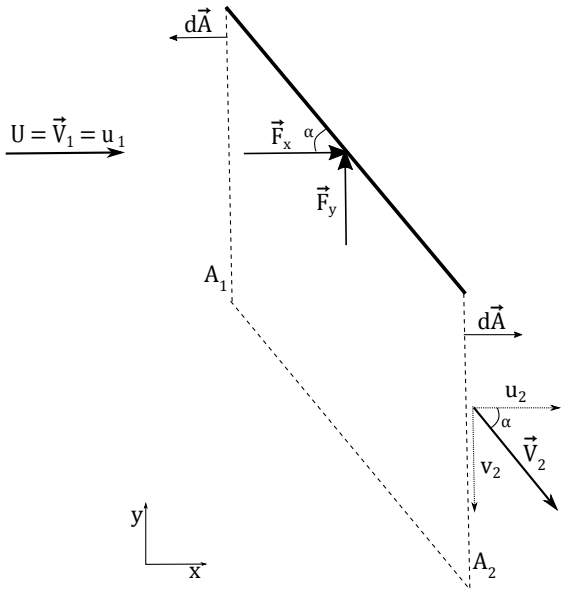

Figure 2: Control volume for a lamella

3.2 Conservation of mass

Now that a control volume is defined, mass balance equations can be formulated. In words, the conservation of mass principle is given by *change of mass in control volume in time = net influx of mass.* Using equations, according to ([2]) this is written as

$$\frac{\partial}{\partial t}\int_{CV}\rho dVol = -\int_{CS}\rho\vec{V}\cdot d\vec{A} \tag{21}$$

where ρ, Vol and $\vec{V}$ are the density, volume and velocity of the fluid respectively and A is a control surface. Furthermore, CV stands for control volume and CS stands for control surface.

It is assumed that the flow is steady (velocity, pressure and cross section of the fluid do not change with time), which causes $\frac{\partial}{\partial t} = 0$. Therefore, for steady flow, the mass balance becomes

$$0 = \int_{CS}\rho\vec{V}\cdot d\vec{A} = \int_{CS_1}\rho\vec{V_1}\cdot d\vec{A} + \int_{CS_2}\rho\vec{V_2}\cdot d\vec{A} \tag{22}$$

where the first term on the right side of the equation represents the mass flow into the control volume (through control surface 1) and the second term represents the mass flow out of the control volume (through control surface 2). Since it is assumed that the flow is incompressible,

$$\int_{CS_1}\rho\vec{V_1}\cdot d\vec{A} = \rho\int_{A_1}|\vec{V_1}||d\vec{A}|\cos\theta_1 \tag{23}$$

where θ_1 is the angle between the velocity vector and the normal vector to the control surface. Since at control surface 1, $\theta_1 = 180°$ (note that this angle can be different if the angle of the "incoming flow" is different) and it is assumed that the flow is uniform,

$$\rho \int_{CS_1} |\vec{V_1}||d\vec{A}| \cos\theta_1 = -\rho u_1 A_1 \tag{24}$$

where u_1 is the x-component of the inflow velocity. Similarly, for CS_2 the following holds:

$$\int_{CS_2} \rho \vec{V_2} \cdot d\vec{A} = \rho A_2 |\vec{V_2}| \cos\theta_2 \tag{25}$$

Here, $\theta_2 \neq 0$ and θ_2 is equal to the angle between the flat plate and the normal vector to control surface 2. Hence, $\theta_2 = \alpha$. The mass balance then becomes

$$0 = -\rho u_1 A_1 + \rho |\vec{V_2}| A_2 \cos\theta_2 = |\vec{V_2}| \cos\alpha - u_1 \tag{26}$$

since $A_1 = A_2$.

From the mass balance, the magnitude of the outflow velocity $|\vec{V_2}|$ can be found. The direction of $\vec{V_2}$ is already known, since it is assumed to be parallel to the lamella.

$$|\vec{V_2}| = \frac{u_1}{\cos\alpha} \tag{27}$$

We are interested in the mass flow rate through both control surfaces. The mass flow rate into the control volume, $\dot{m}_1$, is given by writing out equations (23) and (24),

$$\dot{m}_1 = \int_{CS_1} \rho \vec{V} \cdot d\vec{A} = -\rho u_1 A_1 = -\rho A_{plate} u_1 \sin\alpha \tag{28}$$

The mass flow rate out of the control volume, $\dot{m}_2$, is given by writing out equation (25) and using equation (27),

$$\dot{m}_2 = \int_{CS_2} \rho \vec{V} \cdot d\vec{A} = \rho |\vec{V_2}| A_2 \cos\theta_2 = \rho A_{plate} |\vec{V_2}| \cos\alpha \sin\alpha = \rho A_{plate} u_1 \sin\alpha \tag{29}$$

Note that the sign difference between equations (28) and (29) is because flow out of the control volume is considered positive and flow into the control volume is considered negative. The mass flow rate is the same for the incoming flow as for the outgoing flow. The mass flow rate of the inviscid fluid past the lamella is given by

$$\dot{m}_{plate} = \rho A_{plate} u_1 \sin\alpha \tag{30}$$

where u_1 is the x-component of the upstream velocity (which in this case only has an x-component)

3.3 Momentum balance

Now that the flow velocity behind the lamellae is determined, the integral momentum balance equations will be used to determine the forces on the lamella. Firstly, the momentum balance will be drafted for inviscid flow. Next, viscous flow will be considered, which adds drag forces to the equation.

3.3.1 Inviscid flow

In [2], it is given that the control volume formulation of Newton's second law for a nonaccelerating control volume is given by

$$\vec{F} = \frac{\partial}{\partial t} \int_{CV} \vec{V} \rho dVol + \int_{CS} \vec{V} \rho \vec{V} \cdot d\vec{A} \tag{31}$$

This equation states that the total force (due to surface and body forces) acting on the control volume leads to a rate of change of momentum within the control volume (the volume integral) and/or a net rate at which momentum is leaving the control volume through the control surface. Note that for steady flow, $\frac{\partial}{\partial t} = 0$. Hence, the momentum balance is reduced to

$$\vec{F} = \int_{CS} \vec{V} \rho \vec{V} \cdot d\vec{A} \tag{32}$$

Similarly as for the mass balance, this can be written as

$$\vec{F} = \int_{CS} \vec{V} \rho \vec{V} \cdot d\vec{A} = \int_{CS_1} \vec{V} \rho \vec{V} \cdot d\vec{A} + \int_{CS_2} \vec{V} \rho \vec{V} \cdot d\vec{A} \tag{33}$$

Now let u and v be the components of the velocity $\vec{V}$ in respectively the x- and y-direction. The momentum equation (32) is a vector equation that can be written using the following two scalar components:

$$\vec{F}_x = \int_{CS} u \rho \vec{V} \cdot d\vec{A} \tag{34}$$

$$\vec{F}_y = \int_{CS} v \rho \vec{V} \cdot d\vec{A} \tag{35}$$

where u and v are the x- and y-components of the flow velocity, respectively. So the force on the control volume in the x-direction is given by the expression on the right side in equation (34). The force on the control volume in the y-direction is given by the expression on the right side of the equation (35). The two force components above can be written as

$$\vec{F}_x = \int_{CS_1} u_1 \rho \vec{V}_1 \cdot d\vec{A} + \int_{CS_2} u_2 \rho \vec{V}_2 \cdot d\vec{A} \tag{36}$$

$$\vec{F}_y = \int_{CS_1} v_1 \rho \vec{V}_1 \cdot d\vec{A} + \int_{CS_2} v_2 \rho \vec{V}_2 \cdot d\vec{A} \tag{37}$$

where u_1 and u_2 are the x-components and v_1 and v_2 are the y-components of the flow velocity at A_1 and A_2, respectively. It is trivial that $u_1 = |\vec{V_1}|$, $v_1 = 0$, $u_2 = |\vec{V_2}| \cos\alpha = u_1$ and $v_2 = |\vec{V_2}| \sin\alpha = u_1 \tan\alpha$. Similarly as for the mass balance, (36) and (37) can be written as

$$\int_{CS_1} u_1 \rho \vec{V_1} \cdot d\vec{A} = \rho u_1 \int_{A_1} |\vec{V_1}| \cos\theta_1 |d\vec{A}| = -\rho u_1^2 A_1$$
$$\int_{CS_2} u_2 \rho \vec{V_2} \cdot d\vec{A} = \rho u_2 \int_{A_2} |\vec{V_2}| \cos\theta_2 |d\vec{A}| = \rho u_2 u_1 A_2 = \rho u_1^2 A_2$$
$$\int_{CS_1} v_1 \rho \vec{V_1} \cdot d\vec{A} = 0$$
$$\int_{CS_2} v_2 \rho \vec{V_2} \cdot d\vec{A} = \rho v_2 \int_{A_2} |\vec{V_2}| \cos\theta_2 |d\vec{A}| = \rho v_2 u_1 A_2 = \rho u_1^2 \tan\alpha A_2$$

Hence,

$$\vec{F_x} = -\rho u_1^2 A_1 + \rho u_1^2 A_2 \tag{38}$$
$$\vec{F_y} = \rho u_1 v_2 A_2 \tag{39}$$

Implementing $A_1 = A_2 = A_{screen} \sin\alpha$ into equations (38) and (39) gives

$$\vec{F_x} = -\rho u_1^2 A_{plate} \sin\alpha + \rho u_1^2 A_{plate} \sin\alpha = 0 \tag{40}$$
$$\vec{F_y} = \rho u_1 A_{plate} \sin\alpha v_2 \tag{41}$$

Hence, there is no force in the x-direction. The reason for this is that drag forces are not considered since the fluid is assumed to be inviscid. The case where drag forces are being considered will now be investigated.

3.3.2 Viscous flow

A viscous fluid moving over a submerged flat plate (the lamella) exerts a drag force on the plate, according to [2]. The drag force consists of two components: friction drag and pressure drag. The direction of the drag force is parallel to the direction of relative motion, so the direction of the flow. Pressure drag is the drag force due to pressure difference between in front of and behind the lamella. Friction drag is caused by friction between the fluid and the lamella. Since we are considering an inclined plate, both pressure and friction contribute to the total drag.

The total drag force is given by

$$\vec{F_D} = \vec{F_x} = C_D \frac{1}{2} \rho u_1^2 A_1 \tag{42}$$

where C_D is the drag coefficient, which depends on the Reynolds number and the inclination angle of the lamella. For viscous flow, the force on the lamella in the x-direction is given by equation (42) and the force in the y-direction is given by equation (41).

3.4 Momentum transfer for one lamella

Momentum is being transferred to the rotorarm through the lamellae, but not directly to the lamellae. Therefore, the force that influences the momentum transfer is the force perpendicular to the rotorarm. According to [2], the momentum transfer is then given by

$$\Delta p = \int_t \vec{F}_{\perp,plate} dt \tag{43}$$

Now, the force perpendicular to the rotorarm has to be found. Recall that the forces in the x- and y-direction are given by:

$$\vec{F}_x = \frac{1}{2} C_D \rho u_1^2 A_{plate} \sin\alpha \quad \text{and} \quad \vec{F}_y = \rho u_1^2 \tan\alpha A_{plate} \sin\alpha \tag{44}$$

where C_D is the drag coefficient, u_1 is the (x-component of the) upstream velocity, A_{plate} is the area of the lamella and α is the inclination angle of the lamella.

Let the angle between the upstream flow velocity U and the rotorarm be β. Then the component of $\vec{F}_x$ perpendicular to the rotorarm is given by $\vec{F}_x \sin\beta$ and the component of $\vec{F}_y$ perpendicular to the rotorarm is given by $\vec{F}_y \cos\beta$. Hence,

$$\vec{F}_{\perp,x} = \vec{F}_x \sin\beta = \frac{1}{2} C_D \rho u_1^2 A_{plate} \sin\alpha \sin\beta \tag{45}$$

$$\vec{F}_{\perp,y} = \vec{F}_y \cos\beta = \rho u_1^2 \tan\alpha A_{plate} \sin\alpha \cos\beta \tag{46}$$

Adding these together gives the total force perpendicular to the rotorarm:

$$\vec{F}_{\perp,plate} = \vec{F}_{\perp,x} + \vec{F}_{\perp,y} = \rho u_1^2 A_{plate} \sin\alpha \left(\frac{1}{2} C_D \sin\beta + \tan\alpha \cos\beta \right) \tag{47}$$

The force in equation (47) is the force that contributes to the momentum transfer Δp. The momentum transfer to the rotorarm (containing one lamella) is then given by

$$\Delta p = \vec{F}_{\perp,plate} \cdot t = \rho u_1^2 A_{plate} \sin\alpha \left(\frac{1}{2} C_D \sin\beta + \tan\alpha \cos\beta \right) \cdot t \tag{48}$$

where t is the time for which the force works on the rotorarm. Note that when for example angle α or β depends on the time t, the integrand $\vec{F}_{\perp,plate}$ needs to be integrated attentively. The momentum transfer to the rotorarm containing several lamellae can now be determined.

3.5 Momentum transfer for several lamellae

To determine the momentum transfer to a rotorarm containing several lamellae, we need one control volume. This control volume consists of the added control volumes of the separate lamellae. The rotorarm consists of 12 lamellae. The lamellae are placed on the rotorarm as shown in Figure 3. It will be assumed that when the lamellae are opened, there will be open spaces between the separate control volumes where no momentum is transferred. Therefore, these spaces will not be implemented into our model. If the spaces in between the lamellae are filled by some sort of plate, the added momentum transfer can be added to the model. For 12 lamellae, with empty spaces in between, the force perpendicular to the rotorarm is given by

$$\vec{F}_{\perp,plates} = \rho u_1^2 A_{plate} \sin\alpha \left(6C_D \sin\beta + 12 \tan\alpha \cos\beta\right) \cdot t \tag{49}$$

Note that the result of adding the control volumes is a significantly simplified flow, since in reality the flows past the different lamellae will influence each other.

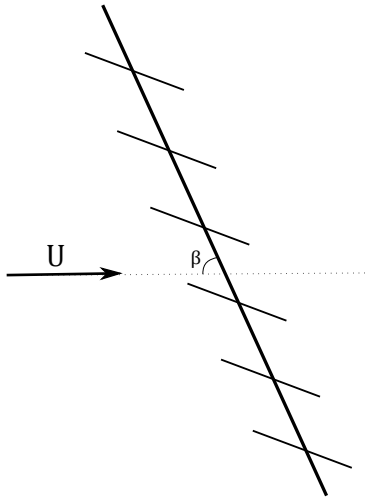

Figure 3: Rotorarm containing lamellae

4 Physical flow through a porous screen

The aim of this research is to see if the lamellae on the rotorarm can be replaced by porous screens. We want to be able to choose the porosity of such a screen such that the mass flow through the sets of lamellae matches the mass flow through the porous screen. Additionally, we want the momentum transfer to the lamellae to match the momentum transfer to the porous screen. In this chapter, the physical phenomenon of flow through a porous screen will be discussed. In the following chapter, a porous screen model will be formulated that can be compared to the lamellae model. According to [5], a porous screen influences a flow in two ways: by reduction of the static pressure across the screen and by deflection of the streamlines towards the normal to the screen. These phenomenons will be investigated in this chapter.

4.1 Porosity

The screen porosity is represented by a dimensionless parameter n, defined as the ratio of open to total aperture area. This parameter can be determined in the following way ([1]):

$$n = \frac{A_{open,ape}}{A_{total,ape}} = \frac{\left(\frac{1}{m} - d\right)^2}{\frac{1}{m^2}} = (1 - md)^2 = (1 - m_1 d_1)(1 - m_2 d_2)$$

where $A_{open,ape}$ is the open area of an aperture, $A_{total,ape}$ is the total area of one aperture, m_1 is the height of the aperture, m_2 is the width of the aperture, d_1 is the diameter of the horizontal wire and d_2 is the diameter of the vertical wire. It is assumed that the porosity n is constant throughout the screen. The open and the closed area of the porous screen can now be determined and they are given by

$$A_{open} = nA_{screen} \quad \text{and} \quad A_{closed} = A_{screen} - A_{open} = (1 - n) A_{screen}$$

where A_{screen} is the total area of the porous screen.

4.2 Pressure drop

Due to the porous screen, there will be a static pressure drop. A general equation for the pressure drop across the screen is given in [1] and [4]. This equation is applicable for incompressible (fluid) flow through woven wire and cloth screens for the wire Reynolds number range of $0.0001 \leq Re_d \leq 10,000$. The wire Reynolds number is based on the average velocity (U), the wire diameter (d) and the kinematic viscosity (ν) of the fluid: $Re_d = \frac{Ud}{\nu}$.

In [4], many previous attempts to determine the incompressible flow pressure drop coefficient K_θ in terms of the screen pressure drop ΔP and upstream velocity U (velocity of the fluid as it approaches the porous screen) are examined.

It is concluded that the pressure drop across the porous screen, ΔP, can be determined using

$$\Delta P = \frac{1}{2} K \rho U^2 \tag{50}$$

where K is the resistance coefficient. According to [4], K can be expressed using two components: a function of the screen porosity, G_n, and a function of the Reynolds number, $f(Re_d)$. Several possible G_n were therefore examined and $G_n = \frac{1-n^2}{n}$ provided the best correlation to the data. In [1], it is given that hence the general expression for K that was found is

$$K = \cos^2\theta \left(\frac{1-n^2}{n^2} \right) f\left(Re_d\right) \tag{51}$$

where $\theta = \frac{\pi}{2} - \alpha$ and α is the inclination angle of the porous screen (the angle between the upstream flow velocity and the porous screen).

According to [1], the function $f(Re_d)$ has evolved to the following expression for flow normal to any screen:

$$f(Re_d) = \frac{C_1}{Re_d} + \frac{C_2}{\log\left(Re_d + 1.25\right)} + C_3 \log\left(Re_d\right) \tag{52}$$

where $C_1 \approx 7.0$, $C_2 \approx 0.9$, $C_3 \approx 0.05$ turned out to be the best fit to the data obtained from experiments. Equation (52) is also used in [5]. It is argued that this model is used since it is based on several earlier models and experiments and it covers a wide Re_d-range.

It is trivial that the expression for K_0 is given by

$$K_0 = K(\theta = 0) = 1 \cdot \left(\frac{1-n^2}{n^2} \right) f(Re_d) \tag{53}$$

Hence,

$$K_0 = \left(\frac{7.0}{Re_d} + \frac{0.9}{\log\left(Re_d + 1.25\right)} + 0.05 \log\left(Re_d\right) \right) \left(\frac{1-n^2}{n^2} \right), \quad 10^{-4} < Re_d < 10^4 \tag{54}$$

Combining (51) and (54), it can easily be seen that

$$K = K_0 \cos^2\theta \tag{55}$$

This is indeed confirmed in [5] and [6]. Admittedly, equation (55) is in [6] confirmed to hold for inclination angles $\alpha \geq 45°$. However, in [5] it is assumed that equation (55) is also applicable for small values of α, given that the Reynolds number dependency of K_0 is properly accounted for, which it is. The formulas for K_0 and K are in principle independent of mesh geometry, but mostly square meshes are used in the measurements and experiments that are done to determine them.

Implementing (55) in (50) gives the following expression for the pressure drop:

$$\Delta P = \frac{1}{2} K_0 \cos^2\theta \rho U^2 \tag{56}$$

where K_0 is given by equation (54), θ is the angle between the normal to the porous screen and the flow velocity (hence, $\theta = \frac{\pi}{2} - \alpha$), ρ is the density of the water and U is the upstream flow velocity.

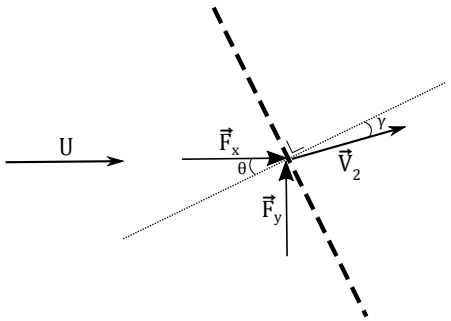

Figure 4: Forces and angles for porous screen

4.3 Deflection

Under influence of the porous screen in the flow, streamlines will be deflected. Deflection of streamlines implies a tangential force due to change of momentum. According to [6], the tangential stress coefficient T_γ is given by

$$T_\gamma(\theta) = \frac{\tau}{\frac{1}{2}\rho U^2} = 2\cos^2\theta\left[\tan(\theta) - \tan\gamma\right], \quad 0 < \gamma < \theta \tag{57}$$

where τ is the tangential stress and γ is the deflection. In [7], it is determined that the deflection γ is given by

$$\gamma = \tan^{-1}\left[\Delta \tan(\theta)\right], \quad \text{where} \tag{58}$$

$$\Delta = \left[\left(\frac{K_0}{4}\right)^2 + 1\right]^{1/2} - \frac{K_0}{4}, \quad 0 < \gamma \leq \theta \tag{59}$$

Since K_0 is known, all variables in the expression for Δ are known. Since θ is also known, the deflection γ can be determined. The expression for T_γ is derived from the basic momentum equations, so it has general validity. For the derivation of γ however, it was assumed in [7] that only twines parallel to the axis of deflection contributed. Therefore, equation (57) has more limited accuracy.

Using γ, the fluid velocity behind the screen, $\vec{V}_2$, can be found. This velocity is given by

$$\vec{V}_2 = U\cos(\theta - \gamma) \tag{60}$$

This expression for the velocity can be used in the next section to determine the forces on the porous screen.

4.4 Forces on a porous screen

The tangential stress T_γ is of course parallel to the screen. However, according to [5], it only includes tangential stress due to deflection. In reality, there is also frictional stress along the screen. This frictional stress is proportional to the square of the flow velocity component parallel to the screen. In equation (60), it is given that the absolute velocity across the screen for a flow passing at an angle γ to the normal is $\vec{V_2} = U\cos(\theta - \gamma)$. The velocity component parallel to the screen is then given by $U\cos(\theta-\gamma)\cos\left(\frac{\pi}{2}-\gamma\right)$. Hence, the total tangential force coefficient will be of the form $T_\gamma + T_f\cos^2(\theta-\gamma)\cos^2\left(\frac{\pi}{2}-\gamma\right)$.

The force coefficients associated with the flow towards the screen are K for the force normal to the screen and $T_\gamma + T_f\cos^2(\theta-\gamma)\cos^2\left(\frac{\pi}{2}-\gamma\right)$ for the force tangential to the screen. The force in the x-direction on the inclined screen can now be expressed in the following way according to [5]:

$$\vec{F_x} = \frac{1}{2}\rho U^2 A_{screen}\left(K\cos\theta + \left(T_\gamma + T_f\cos^2(\theta-\gamma)\cos^2\left(\frac{\pi}{2}-\gamma\right)\right)\sin\theta\right) \quad (61)$$

The normal force coefficient C_N can also be used to express $\vec{F_x}$. According to [5], several models exist for C_N as a function of pressure drop. The one that is used in this report is

$$C_N(K) = \frac{2}{K}\left(K + 1 - \sqrt{2K+1}\right) \quad (62)$$

since this model compares well with measurements presented for values of K up to 10^2. The force F_x is then given by

$$\vec{F_x} = \frac{1}{2}\rho U^2 A_{screen}\left(C_N(K)\cos\theta + \left(T_\gamma + T_f\cos^2(\theta-\gamma)\cos^2\left(\frac{\pi}{2}-\gamma\right)\right)\sin\theta\right) \quad (63)$$

The force component in the y-direction, F_y, is in [5] given by

$$\vec{F_y} = \frac{1}{2}C_L\rho U^2 A_0 \quad (64)$$

where

$$C_L = C_N(K)\tan\theta - \left(T_\gamma + T_f\cos^2(\theta-\gamma)\cos^2\left(\frac{\pi}{2}-\gamma\right)\right) \quad (65)$$

Hence,

$$\vec{F_y} = \frac{1}{2}\rho U^2 A_0\left(C_N(K)\tan\theta - \left(T_\gamma + T_f\cos^2(\theta-\gamma)\cos^2\left(\frac{\pi}{2}-\gamma\right)\right)\right) \quad (66)$$

where A_0 is the projected area of the inclined screen, given by

$$A_0 = A_{screen} cos\theta$$

Now that the forces in the x- and y-direction are found, the resultant force perpendicular to the porous screen can be found:

$$\vec{F}_\perp = F_x \cos\theta + F_y \sin\theta \tag{67}$$

where

$$\vec{F}_x \cos\theta = \frac{1}{2}\rho U^2 A_{screen} \cos\theta \left(C_N(K) \cos\theta + \left(T_\gamma + T_f \cos^2(\theta - \gamma) \cos^2\left(\frac{\pi}{2} - \gamma\right)\right) \sin\theta \right)$$

$$\vec{F}_y \sin\theta = \frac{1}{2}\rho U^2 A_0 \sin\theta \left(C_N(K) \tan\theta - \left(T_\gamma + T_f \cos^2(\theta - \gamma) \cos^2\left(\frac{\pi}{2} - \gamma\right)\right)\right)$$

Implementing the expression for A_0, we get

$$\vec{F}_y \sin\theta = \frac{1}{2}\rho U^2 A_{screen} \cos\theta \sin\theta \left(C_N(K) \tan\theta - \left(T_\gamma + T_f \cos^2(\theta - \gamma) \cos^2\left(\frac{\pi}{2} - \gamma\right)\right)\right)$$

Hence, equation (67) can be simplified to

$$\vec{F}_\perp = \frac{1}{2}\rho U^2 A_{screen} \cos\theta \left((C_N(K) (\cos\theta + \tan\theta \sin\theta)) + T_\gamma (1 - \sin\theta) \right) \tag{68}$$

Since the porous screen is in the same direction as the rotorarm, the force perpendicular to the rotorarm is equal to the force perpendicular to the porous screen. This is the only force that contributes to the momentum transfer and it is given by equation (68). Now that this force is known, first the mass flow through and then the momentum transfer to the porous screen will be determined.

4.5 Mass flow

The mass flow rate ([2]) is given by

$$\dot{m} = \rho U A_{open} \cos\gamma \tag{69}$$

where ρ is the density of the water, A_{open} is the open area of the porous screen, γ is the deflection (so the angle between the normal vector to the porous screen and the flow velocity) and U is the flow velocity of the water. The open area of the porous screen is given by

$$A_{open} = nA_{screen}$$

where A_{screen} is the total area of the porous screen.

4.6 Momentum transfer to a porous screen

The forces given by equations (63), (66) and thus equation (68) are determined for viscous flow. Since the porous screen is in the same direction as the rotorarm, the force perpendicular to the porous screen is equal to the force perpendicular to the rotorarm. Therefore, the force perpendicular to the porous screen is the netto force that contributes to the momentum transfer. This force is thus given by equation (68):

$$\vec{F}_{\perp,screen} = \frac{1}{2}\rho U^2 A_{screen} \cos\theta \left((C_N(K) \left(\cos\theta + \tan\theta \sin\theta\right)) + T_\gamma \left(1 - \sin\theta\right)\right)$$

where θ is the angle between the normal vector to the porous screen and the direction of the upstream flow velocity U. Since the force on the porous screen is equal to the momentum transfer per unit time, i.e. $\vec{F} = \frac{\partial p}{\partial t}$, the momentum transfer from the fluid to the porous screen is given by

$$\Delta p = \int_t \vec{F}_{\perp,screen} dt \tag{70}$$

where t is the time over which the force works on the porous screen. Note that when for example θ depends on time t, this integrand should be integrated with care. But in this case, since no term in the expression for $\vec{F}_{\perp,screen}$ depends on t, this gives

$$\Delta p = \left(\frac{1}{2}\rho U^2 A_{screen} \cos\theta \left((C_N(K) \left(\cos\theta + \tan\theta \sin\theta\right)) + T_\gamma \left(1 - \sin\theta\right)\right) \right) \cdot t \tag{71}$$

This is the expression for the linear momentum transfer. If we want to consider the angular momentum, this expression has to be multiplied by the length of the arm ([2]). The length of the arm is in this case the width of the porous screen.

Thus, the physical momentum transfer to the rotorarm containing a porous screen is given by equation (71). This result tells us what happens physically when a fluid (water) flows through a porous screen. However, we want the mass flow and momentum transfer for the porous screen model to be similar or equal to the mass flow and momentum transfer for the lamellae model. To get this result, we need some more information, which will be discussed in the next chapters.

5 Mass- and momentum balances for a porous screen

The results in the previous chapter are mainly physical, since for example the coefficients C_1, C_2 and C_3 in the expression for K are found through experiments. However, the goal of this research is to find the relation between the porosity of the porous screen and the opening angle of the lamellae. Therefore, mass- and momentum balances for flow through a porous screen will be drafted in this chapter. Then, since we want the porous screen to have the same effect on the flow as the lamella, a relation between the porosity of the screen and the opening angle of the lamella can be found in the next chapter. This relation will be verified numerically. To be able to check the result numerically, a convenient control volume has to be used. This control volume and the mass- and momentum balances will be stated in this chapter.

5.1 Control volume

The numerical model that will be used consists of a vertical wall containing an opening. For the porous screen model, a porous screen is placed in said opening. The numerical model will be used to compare one lamella to a porous screen of the same size, instead of several lamellae. Note that the porous screen is pinned to the wall, so it is in the same position and direction as the wall, which is vertical (y-direction). To simplify the process of solving the problem, the control volume is just a rectangular shape around the porous screen. The left control surface (CS_1) is equal to the porous screen area and the right control surface (CS_2). The control volume is shown in Figure 5.

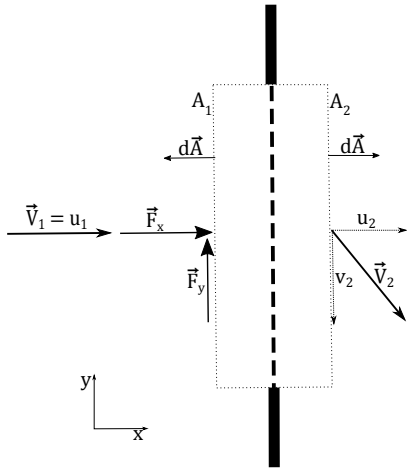

Figure 5: Control volume for the porous screen in the numerical model

5.2 Source term

We essentially want the porous screen to have the same effect on the flow as the lamella. Hence, a change of velocity direction should be implemented. This change of velocity direction due to the porous screen suggests that some force is added (in the porous screen) that makes the fluid flow change direction. In the numerical model, source term $\vec{S}$ will be used to describe this force. This source term is given by

$$\vec{S} = -\mu D\vec{U} \tag{72}$$

where μ is the viscosity of the water, D is a tensor that describes the Darcy coefficients and U is the flow velocity through the porous screen. This term is negative because it is representing a force the screen exerts on the flow, instead of a force the flow exerts on the screen.

The components of the flow velocity U in x- and y-direction are respectively $U\cos\alpha$ and $U\sin\alpha$. Hence, U is given by

$$\vec{U} = \begin{pmatrix} U\cos\alpha \\ U\sin\alpha \end{pmatrix}$$

The Darcy coefficients in tensor D represent a linear relation between the source term S and the velocity U ([11]). Therefore, the matrix forming tensor D should be positive (semi-)definite, since such a matrix represents a linear relation. Tensor D is a 2×2-matrix since two dimensions are being considered. The matrix should also be (real and) symmetric since we want the eigenvalues to be real. A symmetric matrix D is given by

$$D = R^T \tilde{D} R \tag{73}$$

where R is a rotation matrix and $\tilde{D}$ can be a diagonal matrix of the form

$$\tilde{D} = \begin{pmatrix} d_1 & 0 \\ 0 & d_2 \end{pmatrix}$$

The rotation matrix R is given by

$$R = \begin{pmatrix} \cos\alpha & \sin\alpha \\ -\sin\alpha & \cos\alpha \end{pmatrix}$$

since we have a clockwise rotation of angle α. The fluid velocity vector should rotate clockwise with angle α, since we want the change in direction of the fluid velocity to be the same as for the lamella. For rotation matrices it holds that $R^T = R^{-1}$ and thus

$$D^T = \left(R^{-1}\tilde{D}R\right)^T = \left(R^T\tilde{D}R\right)^T = R^T\tilde{D}R = D$$

Hence, D is indeed symmetric.

The source term $\vec{S}$ is now given by

$$\vec{S} = -\mu R^T \tilde{D} R \vec{U}$$

where

$$R^T \tilde{D} R = \begin{pmatrix} d_1 \cos^2\alpha + d_2 \sin^2\alpha & \cos\alpha \sin\alpha (d_1 - d_2) \\ \cos\alpha \sin\alpha (d_1 - d_2) & d_1 \sin^2\alpha + d_2 \cos^2\alpha \end{pmatrix}$$

Writing the source term $\vec{S}$ then gives

$$\vec{S} = \begin{pmatrix} S_x \\ S_y \end{pmatrix} = -\mu U \begin{pmatrix} d_1 \cos^3\alpha + d_1 \cos\alpha \sin\alpha \\ d_1 \sin^3\alpha + d_1 \cos^2\alpha \sin\alpha \end{pmatrix}$$

Hence, d_2 is a free variable. We let $d_2 = 0$ and if we then denote d_1 by just d, we get the tensor D:

$$D = R^T \tilde{D} R = \begin{pmatrix} \cos\alpha & -\sin\alpha \\ \sin\alpha & \cos\alpha \end{pmatrix} \begin{pmatrix} d & 0 \\ 0 & 0 \end{pmatrix} \begin{pmatrix} \cos\alpha & \sin\alpha \\ -\sin\alpha & \cos\alpha \end{pmatrix} \tag{74}$$

The eigenvalues of tensor D are given by $\lambda_1 = d$ and $\lambda_2 = 0$. Since we want D to be positive semi-definite, $\lambda_1 = d$ should be positive.

The total forces exerted by the porous screen on the fluid will be determined in the next section. The coefficient d can be determined by letting the forces exerted by the lamella be equal to the forces exerted by the porous screen, which will be done after that.

5.3 Forces

To be able to determine the coefficients of matrix D, the forces exerted by the porous screen on the fluid have to be equal to the forces exerted by the lamella in both the x- and y-direction. The forces in equation (44) are exerted by the flow on the lamella. The source term S represents the force exerted by the porous screen on the flow (hence, in the opposite direction). Therefore, to be able to compare them, the forces in equations (44) have to change sign. Hence,

$$\vec{F}_{plate,num} = \begin{pmatrix} \vec{F}_{x,plate,num} \\ \vec{F}_{y,plate,num} \end{pmatrix} = \begin{pmatrix} -\frac{1}{2} C_D \rho u_1^2 A_{plate} \sin\alpha \\ -\rho u_1^2 \tan\alpha A_{plate} \sin\alpha \end{pmatrix} \tag{75}$$

The forces exerted by the screen in the x- and y-direction are given by

$$\vec{F}_{screen,num} = \begin{pmatrix} \vec{F}_{x,screen,num} \\ \vec{F}_{y,screen,num} \end{pmatrix} = \begin{pmatrix} -\int_{CS_1} u_1 \rho \vec{V}_1 \cdot d\vec{A} + S_{x,num} \\ -\int_{CS_1} v_1 \rho \vec{V}_1 \cdot d\vec{A} + S_{y,num} \end{pmatrix} \tag{76}$$

since the force at CS_2 can be replaced by the source term. Since we want the porous screen to have the same effect on the water flow as the lamella, the

velocity U in the source term has to be the same velocity as $\vec{V}_2$ for the lamella. Hence,

$$\vec{U} = \begin{pmatrix} u_2 \\ v_2 \end{pmatrix} = \begin{pmatrix} u_1 \\ u_1 \tan\alpha \end{pmatrix} \tag{77}$$

Therefore, the components of the source term become

$$S = \begin{pmatrix} S_{x,num} \\ S_{y,num} \end{pmatrix} = -\mu \begin{pmatrix} du_1 \\ du_1 \left(\cos\alpha \sin\alpha + \tan\alpha \sin^2\alpha\right) \end{pmatrix} \tag{78}$$

Also solving the integrals in (76) gives the result

$$\vec{F}_{screen,num} = \begin{pmatrix} \vec{F}_{x,screen,num} \\ \vec{F}_{y,screen,num} \end{pmatrix} = \begin{pmatrix} \rho u_1^2 (1-n) A_{screen} - \mu d u_1 \\ -\mu d u_1 \left(\cos\alpha \sin\alpha + \tan\alpha \sin^2\alpha\right) \end{pmatrix} \tag{79}$$

Now that the expressions for the forces in the x- and y-direction of both the lamella model and the porous screen model are determined, they can be used to find the coefficient d of the Darcy tensor D.

5.4 Finding coefficient d

Expressions for d can be found by letting $\vec{F}_{plate,num}$ be equal to $\vec{F}_{screen,num}$. The system that needs to be solved is then given by

$$\begin{pmatrix} -\frac{1}{2} C_D \rho u_1^2 A_{plate} \sin\alpha \\ -\rho u_1^2 \tan\alpha A_{plate} \sin\alpha \end{pmatrix} = \begin{pmatrix} \rho u_1^2 (1-n) A_{screen} - \mu d u_1 \\ -\mu d u_1 \left(\cos\alpha \sin\alpha + \tan\alpha \sin^2\alpha\right) \end{pmatrix} \tag{80}$$

Only one area is used in the whole system since $A_{screen} = A_{plate}$, so from now on it will be denoted by A. Note that the first equation gives

$$d = \frac{\rho A}{\mu} \left(\frac{1}{2} C_D u_1 \sin\alpha + u_1 (1-n) \right) \tag{81}$$

and the second equation gives

$$d = \frac{\rho A}{\mu} \left(\frac{u_1 \tan\alpha \sin\alpha}{\cos\alpha \sin\alpha + \tan\alpha \sin^2\alpha} \right) = \frac{\rho A}{\mu} \left(u_1 \sin\alpha \right) \tag{82}$$

Since d has to be positive (D has to be a positive semi-definite matrix), we should have that

$$\frac{\rho A}{\mu} \left(\frac{1}{2} C_D u_1 \sin\alpha + u_1 (1-n) \right) > 0 \quad \text{and} \quad \frac{\rho A}{\mu} \left(u_1 \sin\alpha \right) > 0$$

Density ρ, area A and viscosity μ are all positive and so is u_1 (we assume that the fluid does flow towards the screen). For the porosity n it holds that $0 < n < 1$ and thus, $0 < 1 - n < 1$. Also note that for the range of α, which is $0 < \alpha < \pi$, $\sin\alpha$ is always positive. Hence, both expressions for d are always positive and

thus matrix D is positive semi-definite.

The force exerted by the porous screen on the fluid is given by

$$\vec{F}_{screen,num} = \begin{pmatrix} \rho u_1^2 \left(1-n\right) A_{screen} \\ 0 \end{pmatrix} + \vec{S} \tag{83}$$

where source term $\vec{S}$ is given by $-\mu R^T \tilde{D} R \vec{U}$ with

$$R = \begin{pmatrix} \cos\alpha & \sin\alpha \\ -\sin\alpha & \cos\alpha \end{pmatrix}, \quad \vec{U} = \begin{pmatrix} u_1 \\ u_1 \tan\alpha \end{pmatrix}$$

and

$$\tilde{D} = \begin{pmatrix} \frac{\rho A}{\mu}\left(\frac{1}{2} C_D u_1 \sin\alpha + u_1(1-n)\right) & 0 \\ 0 & 0 \end{pmatrix} = \begin{pmatrix} \frac{\rho A}{\mu} u_1 \sin\alpha & 0 \\ 0 & 0 \end{pmatrix}$$

Hence, equation (83) gives the forces exerted by the porous screen on the fluid in the x- and the y-direction. From this, the relation between the porosity n of the porous screen and the opening angle α of the lamella can be determined. This will be done in the next chapter.

6 Relation between porosity and opening angle

The purpose of this research is to investigate whether the porous screen model can be used as an alternative for the lamellae. Hence, a relation has to be found between the porosity n of the porous screen and the opening angle α of the lamella. This will first be done by comparing the mass flow through the porous screen to the mass flow past the lamella. Then, the momentum balances of both the lamella and the porous screen will be used to determine the relation.

6.1 Mass flow

To see if the porous model can be used as an alternative to the lamellae, the mass flow rate will be compared for both models. The mass flow rate past a lamella is given by equation (30). Thus,

$$\dot{m}_{plate} = \rho A_{plate} u_1 \sin\alpha \tag{84}$$

where ρ is the density of the water, A_{plate} is the total area of the lamella, u_1 is the upstream flow velocity (since the flow direction is the x-direction) and α is the angle between the horizontal (x)-direction and the inclined lamella. The mass flow rate through the porous screen used in the numerical model is given by

$$\dot{m}_{screen} = \rho A_{open} u_2 = \rho n A_{screen} u_1 \tag{85}$$

where u_2 is the x-component of the flow velocity behind the screen and A_{open} is the open area of the porous screen which is given by nA_{screen}, where n is the porosity.

If we want the two mass flows to be equal we can write

$$\dot{m}_{plate} = \dot{m}_{screen} \implies \rho A_{plate} u_1 \sin\alpha = \rho n A_{screen} u_1$$

Since $A_{plate} = A_{screen}$, we have

$$n = \sin\alpha$$

Since the mass flow rates depend greatly on the chosen control surfaces, this result was to be expected. As can be seen in equations (84) and (85), the mass flow rates only differ due to the chosen areas. For the porous screen it is assumed that the fluid has to transfer through the screen since there is a closed wall next to it. However, for the lamella model it was assumed that the fluid can flow around the lamella and there is no wall. Comparing the mass flows does not yield a useful result. The momentum balances have to be used to get a real relation between the porosity and the opening angle. Forces exerted by the porous screen will then be compared to forces exerted by the lamella, which will not be influenced by the presence of a wall. The momentum balances also include the drag force, which will probably influence the relation to make it more realistic.

6.2 Momentum transfer

The momentum balances for the porous screen are stated in the previous chapter. To get the forces exerted by the lamella and the porous screen and thus the momentum transfer (since the porous screen is placed vertically) to be equal, both expressions for d in equations (81) and (82) have to be equal. Hence,

$$\frac{\rho A}{\mu}\left(\frac{1}{2}C_D u_1 \sin\alpha + u_1(1-n)\right) = \frac{\rho A}{\mu}\left(u_1 \sin\alpha\right)$$

From this, it follows that the relation between porosity n of the porous screen and opening angle α of the lamella is given by

$$1 - n = \sin\alpha\left(1 - \frac{1}{2}C_D\right) \Rightarrow n = 1 - \sin\alpha\left(1 - \frac{1}{2}C_D\right) \tag{86}$$

Note that C_D has to be smaller than 2 for $(1-n)$ to stay positive. For an (inclined) flat plate in a fluid flow this is indeed the case ([12]).

The relation in equation (86) will now be checked for the extreme cases where $\alpha = \frac{\pi}{2}$ (the lamella is perpendicular to the upstream flow velocity) and $\alpha = 0$ and $\alpha = \pi$ (the lamella is parallel to the upstream flow velocity). It is trivial that the porosity should be minimal (fully closed) for $\alpha = \frac{\pi}{2}$ and maximal for $\alpha = 0$ and $\alpha = \pi$ (fully opened).

$$n\left(\frac{\pi}{2}\right) = 1 - \sin\left(\frac{\pi}{2}\right)\left(1 - \frac{1}{2}C_D\right) = 1 - \left(1 - \frac{1}{2}C_D\right) = \frac{1}{2}C_D$$

$$n\left(0\right) = n\left(\pi\right) = 1 - \sin\left(0\right)\left(1 - \frac{1}{2}C_D\right) = 1$$

So the porosity is indeed maximal for a lamella perpendicular to the flow. According to [12], for a flat plate, the relation between the drag coefficient and the angle of attack (which is the same as the opening angle) is given by

$$C_D \simeq 1.28 \sin\alpha$$

For $0 < \alpha < \pi$ it holds that $0 < \sin\alpha < 1$, so we have that $C_D < 2$. Since $C_D < 2$, the expression for n is always positive. Furthermore, it is admissible that $\frac{1}{2}C_D < n < 1$. Thus, the relation between porosity n and opening angle α is given by equation (86). This relation will now be validated using the numerical model.

7 Numerical model

The analytically found relation between the porosity n and the opening angle α can be verified numerically using OpenFOAM. The model that is used is written by dr. ir. D.R. van der Heul, researcher at the Delft University of Technology. In this research only the rotation matrix R, the diagonal matrix $\tilde{D}$ and thus tensor D will be varied. The goal is to recognize the correct trend in deflection of the flow velocity for different angles α. Tensor D and rotation matrix R both depend on opening angle α of the lamella. For several opening angles α, the effect of the porous screen on the flow (velocity) can be visualised. If this effect, in particular the deflection of flow velocity, is the same as for the lamella, it can be concluded that the tensor D and rotation matrix R are legitimate.

7.1 Results

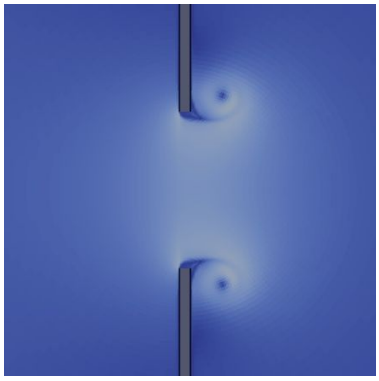

Figure 6: $\alpha = 0$

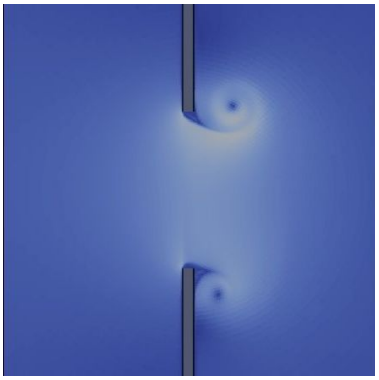

Figure 7: $\alpha = \frac{\pi}{8}$

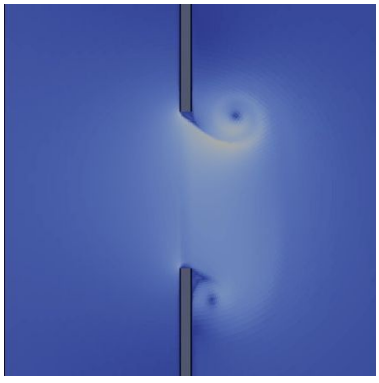

Figure 8: $\alpha = \frac{\pi}{4}$

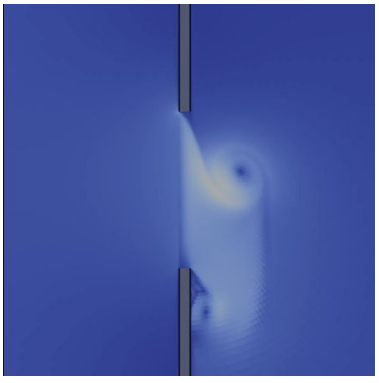

Figure 9: $\alpha = \frac{3\pi}{8}$

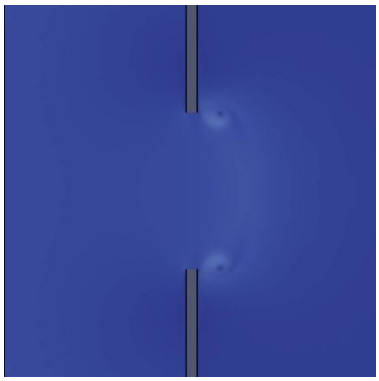

Figure 10: $\alpha = \frac{\pi}{2}$

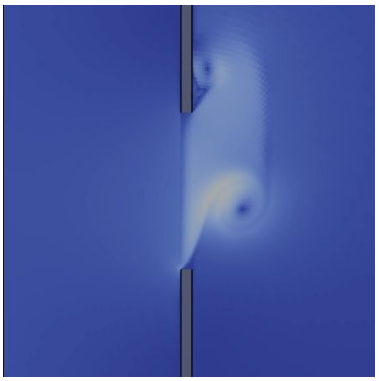

Figure 11: $\alpha = \frac{5\pi}{8}$

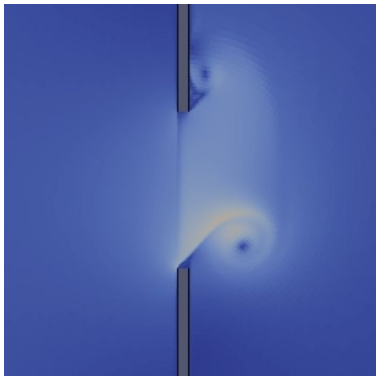

Figure 12: $\alpha = \frac{3\pi}{4}$

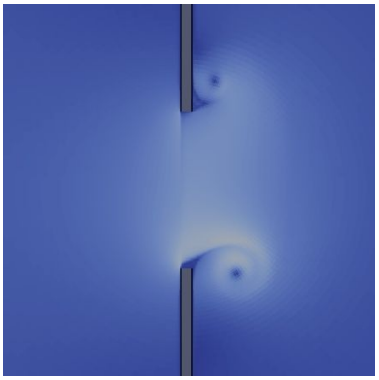

Figure 13: $\alpha = \frac{7\pi}{8}$

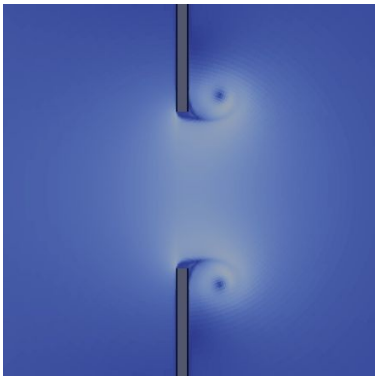

Figure 14: $\alpha = \pi$

7.2 Notes

The author would like to make some remarks regarding the numerical model. Firstly, note that the results in the figures above are the desired results. The figures show the velocity profile around the wall containing a porous screen. The darker the color (blue), the higher the velocity. Note that vortices can be seen, which is a natural occurance, as discussed in the chapter of this report concerning potential flow. The deflection angle of the flow velocity should be the same as for a lamella with opening angle α. For $\alpha = 0$ and $\alpha = \pi$, the flow should not change direction. For $\alpha = \frac{\pi}{2}$, there should be no flow through the screen. For all the other values of α, the direction of the flow velocity should rotate clockwise with angle α. This is indeed the case. However, the following remarks have to be made regarding these results.

As mentioned before, the only factors that are varied in the model are diagonal matrix $\tilde{D}$ and rotation matrix R. The rotation matrix is inserted in the model as two basis vectors instead of a full matrix. Besides, models in OpenFOAM are always three-dimensional. Therefore, both basis vectors contain three elements. Since the analytical model is two-dimensional, the third element will be zero. The basis vectors will then be

$$a_1 = \begin{pmatrix} \cos\alpha \\ -\sin\alpha \\ 0 \end{pmatrix} \quad \text{and} \quad a_2 = \begin{pmatrix} \sin\alpha \\ \cos\alpha \\ 0 \end{pmatrix}$$

Tensor D is inserted into the model by inserting rotation matrix R and diagonal matrix $\tilde{D}$. According to the analytical model and since OpenFOAM uses three-dimensional models, diagonal matrix $\tilde{D}$ should be of the following form:

$$\tilde{D} = \begin{pmatrix} d & 0 & 0 \\ 0 & 0 & 0 \\ 0 & 0 & 0 \end{pmatrix}$$

which can be implemented in the OpenFOAM model in the form $\tilde{D} = (d \quad 0 \quad 0)$. However, inserting this $\tilde{D}$ does not give the correct result. Inserting $\tilde{D}$ of the form $\tilde{D} = (0 \quad d \quad 0)$ does give the desired result. The author of the report and the writer of the numerical model have not yet found an exact explanation for this deviation. For the results above, $\tilde{D} = (0 \quad d \quad 0)$ is used.

The author of the report and the writer of the OpenFOAM model (dr. ir. D.R. Van der Heul, Delft University of Technology) both suspect that OpenFOAM uses a different, alternative conversion from the rotation matrix to the basis vectors. This conclusion was drawn after also running the model for standard basis vectors. It is useful to further investigate this phenomenon before possibly expanding the research.

8 Conclusion

There are several ways of modelling flow past several lamellae (flat plates) two-dimensionally. Determining a potential flow model for uniform potential flow past several flat plates can be done using Schwarz Christoffel mappings and the Schottky-Klein prime function.

In this research, mass- and momentum balances are used to determine the mass flow past and forces on a flat plate. Using the right control volumes, these can also be determined for several lamellae on a rotorarm. The momentum transfer to the rotorarm is given by integrating the force perpendicular to the rotorarm over the time. By including a drag force in the equation and thus considering viscous flow, the model becomes more realistic.

Physically, the consequences of placing a porous screen in a fluid flow are pressure drop across the screen and deflection of the flow velocity. The pressure drop and deflection can be determined. For this, results from experiments are needed. Since we just want the effect of the porous screen to be the same as the effect of the lamellae in the model, the properties of the porous screen do not have to be physically correct. Mass- and momentum balances for the porous screen are therefore considered, which are used to find the conditions that the screen needs to satisfy.

Since the porous screen has to deflect the flow velocity, a source term has to be added to the momentum balance. This source term $\vec{S}$ is of the form $-\mu D\vec{U}$, which gives a linear relation since D represents a Darcy tensor. Since the relation between $\vec{S}$ and $\vec{U}$ needs to be linear, D has to be a positive (semi)definite 2×2 matrix. This matrix D is given by $R^T \tilde{D} R$, where R is a rotation matrix and $\tilde{D}$ is a diagonal matrix of which the first (diagonal) entry is given by coefficient d and the other entries are all zero. After setting the forces exerted by the porous screen equal to the forces exerted by the lamella, $d = \frac{\rho A}{\mu} u_1 \sin\alpha = \frac{\rho A}{\mu}\left(\frac{1}{2} C_D u_1 \sin\alpha + u_1(1-n)\right)$. From this, it can be concluded that the relation between the porosity n of the porous screen and the opening angle α of the lamella is given by

$$n = 1 - \sin\alpha \left(1 - \frac{1}{2} C_D\right)$$

This relation between n and α is not yet validated numerically. The diagonal matrix $\tilde{D}$ and the rotation matrix R are inserted in the numerical model. However, it is suspected that the definition of the rotation matrix in OpenFOAM is different than expected. This can not yet be confirmed. As a consequence, the analytically found $\tilde{D}$ of the form $(d \quad 0 \quad 0)$ does not give the right result. However, $\tilde{D}$ of the form $(0 \quad d \quad 0)$ does give the correct result. Therefore, no conclusion can be drawn from the numerical results until this difference in Darcy tensor D is investigated further.

9 Discussion

Firstly, the difference between the current problem and the real lamellae has to be discussed. The motion of the lamellae in this research is not the same as the motion of the lamellae for the real Oryon watermill. The current problem is more complex since it is assumed that the lamellae are in a fixed position, which causes the flow velocity to deflect. For the real Oryon watermill, the lamellae are able to move under the influence of the hydrodynamic load. In that case, the lamellae will only deflect the flow velocity when they are completely closed. Hence, the current problem is a more generic case than the case where the lamellae are able to move.

The analytical models used in this research represent a simplified view of reality, as is often the case in modelling. For example, it is assumed that the flow velocity changes direction uniformly, which is probably not veracious. Including the drag force makes the result more valid, because it is a physical occurance and it includes the drag coefficient which is determined through physical experiments. The analytical part of this research can be expanded in many ways. The goal would be to make the model more realistic. For example, a potential flow model for uniform potential flow past several lamellae can be determined. Such a model will probably be more accurate than a model using integral mass- and momentum balances, because it would include the influence the lamellae have on each other.

As discussed in the chapter containing the numerical model, further investigation of the OpenFOAM model is needed. For example, we want to know how the rotation matrix should exactly be inserted into the model. Because of the lack of knowledge on this topic, unfortunately no reliable conclusion can be drawn from the numerical model at this moment. To avert this problem, the exact definition of the basis vectors in the OpenFOAM model should be investigated. For now, no conclusion will be drawn about the analytical result based on the numerical results. A useful expansion of the numerical model would for example be to include angles of the rotorarm. In the current model, the porous screen attached to the rotorarm is assumed to be positioned vertically. By including angles, the rotation of the rotorarms can be implemented in the model.

In future research, the scale of the porous screen could be increased. In the current numerical model, one porous screen "replaces" one lamella. It may be possible to model the whole rotorarm as one porous screen. One might be interested in the effects of the watermill downstream. In that case it might even be possible to model the whole watermill using one porous screen containing several different time/position- dependent porous zones. It is evident that the Oryon watermill remains an interesting and inspiring object for further modelling.

References

[1] Brundett, E. *Prediction of Pressure Drop for Incompressible Flow Through Screens*. Department of Mechanical Engineering, University of Waterloo, 1993.

[2] Fox, R.W., McDonald, A.T., Pritchard, P.J., Mitchell, J.W., Leylegian, J.C. *Fluid Mechanics, 9th edition*. John Wiley & Sons (Asia) Pte Ltd, 2016.

[3] Laws, E.M., Livesey, J.L. *Flow through screens*. University of Salford. Annual Reviews Inc, 1978.

[4] Pinker, R.A., Herbert, M.V. *Pressure loss associated with compressible flow through square-mesh wire gauzes*. Journal Mechanical Engineering Science, 1967.

[5] Gjosund, S.H., Enerhaug, B. *Flow through nets and trawls of low porosity*. SINTEF Fisheries and Aquaculture. Ocean Engineering, 2010.

[6] Schubauer, G.B., Spangenberg, W.G., Klebanoff, P.S. *Aerodynamic characteristics of damping screens*. NACA Technical Note No. 2001, 1950.

[7] Gibbings, J.C. *The pyramid gauze diffuser*. Ingenieur-Archiv 42, S 225-233. Springer-Verlag, 1973.

[8] Veldman, A., Velická, A. *Stromingsleer*. Instituut voor Wiskunde en Informatica, Rijksuniversiteit Groningen, 2011.

[9] Crowdy, D.A. *Analytical solutions for uniform flow past multiple cylinders*. Department of Mathematics, Imperial College London. European Journal of Mechanics B/Fluids, 2006.

[10] Crowdy, D. *Schwarz-Christoffel mappings to unbounded multiply connected polygonal regions*. Department of Mathematics, Imperial College London. Math. Proc. Camb. Phil. Soc., 2007.

[11] Zimmermann, R.W. *Flow in Porous Media*. Department of Earth Science and Engineering, Imperial College London. MSc in Petroleum Engineering, 2002-2003.

[12] Hall, N. *Kite Inclination Effects, Lift and Drag* Glenn Research Center, NASA, 2015. https://www.grc.nasa.gov/www/k-12/airplane/kiteincl.html

[13] *Waterkracht-uitvinding maakt kans op innovatieprijs* De Binnenvaartkrant, 2013. http://www.binnenvaartkrant.nl/nieuws/nieuwsitem/waterkracht-uitvinding-maakt-kans-op-innovatieprijs/